PHILOSOPHICAL TRANSACTIONS B

royalsocietypublishing.org/journal/rstb

Research

Cite this article: Vishwakarma M, Thurakkal B, Spatz JP, Das T. 2020 Dynamic heterogeneity influences the leader–follower dynamics during epithelial wound closure. *Phil. Trans. R. Soc. B* **375**: 20190391.
http://dx.doi.org/10.1098/rstb.2019.0391

Accepted: 6 November 2019

One contribution of 14 to a theme issue 'Multi-scale analysis and modelling of collective migration in biological systems'.

Subject Areas:
biophysics

Keywords:
collective cell migration, dynamic heterogeneity, cell density, mechanobiology

Author for correspondence:
Tamal Das
e-mail: tdas@tifrh.res.in

Electronic supplementary material is available online at https://doi.org/10.6084/m9.figshare.c.5025701.

THE ROYAL SOCIETY PUBLISHING

Dynamic heterogeneity influences the leader–follower dynamics during epithelial wound closure

Medhavi Vishwakarma[1,3], Basil Thurakkal[2], Joachim P. Spatz[3,4] and Tamal Das[2]

[1]School of Cellular and Molecular Medicine, University of Bristol, University Walk, Bristol BS8 1TD, UK
[2]TIFR Centre for Interdisciplinary Sciences, Tata Institute of Fundamental Research Hyderabad (TIFR-H), Hyderabad 500046, India
[3]Department of Cellular Biophysics, Max Planck Institute for Medical Research, Heidelberg 69120, Germany
[4]Department of Biophysical Chemistry, University of Heidelberg, Heidelberg 69117, Germany

TD, 0000-0002-6576-5552

Cells of epithelial tissue proliferate and pack together to attain an eventual density homeostasis. As the cell density increases, spatial distribution of velocity and force show striking similarity to the dynamic heterogeneity observed elsewhere in dense granular matter. While the physical nature of this heterogeneity is somewhat known in the epithelial cell monolayer, its biological relevance and precise connection to cell density remain elusive. Relevantly, we had demonstrated how large-scale dynamic heterogeneity in the monolayer stress field in the bulk could critically influence the emergence of leader cells at the wound margin during wound closure, but did not connect the observation to the corresponding cell density. In fact, numerous previous reports had essentially associated long-range force and velocity correlation with either cell density or dynamic heterogeneity, without any generalization. Here, we attempted to unify these two parameters under a single framework and explored their consequence on the dynamics of leader cells, which eventually affected the efficacy of collective migration and wound closure. To this end, we first quantified the dynamic heterogeneity by the peak height of four-point susceptibility. Remarkably, this quantity showed a linear relationship with cell density over many experimental samples. We then varied the heterogeneity, by changing cell density, and found this change altered the number of leader cells at the wound margin. At low heterogeneity, wound closure was slower, with decreased persistence, reduced coordination and disruptive leader–follower interactions. Finally, microscopic characterization of cell–substrate adhesions illustrated how heterogeneity influenced orientations of focal adhesions, affecting coordinated cell movements. Together, these results demonstrate the importance of dynamic heterogeneity in epithelial wound healing.

This article is part of the theme issue 'Multi-scale analysis and modelling of collective migration in biological systems'.

1. Introduction

Epithelial cells mark the inner and outer linings of all the organs of our body, acting as physical barriers that protect the underlying tissues from invasions and infections and that help in the absorption of nutrients from food [1,2]. During organogenesis, cells display multicellular coordination in growth, division and migration [3,4] and eventually attain a homeostatic and jammed state, which they tend to maintain throughout the lifetime of the organism [2,5]. In a physical sense, such a transition is similar to the non-equilibrium glass transition in two ways. First, the individual movements slow down almost to the point of kinetic arrest—a process known as jamming transition. Second, the monolayer exhibits dynamic heterogeneity, meaning while on average, collective

movement slows down with increasing density, relatively unjammed cells display a progressively increasing length scale of movement coordination [6–14]. While there are indications that this jamming–unjamming of epithelial cells may play a critical role in cell density regulation [15] in the pathogenesis of asthma [9], in animal development [16] and in dissemination of tumour cells [17], the biological significance of the associated dynamic heterogeneity remains mostly elusive.

Interestingly, movement coordination of a similar order has been observed during wound healing when cells are required to unjam and perform collective migration to quickly cover the wounded area [18–24]. In this process, special cells known as 'leader cells' migrate at the tips of cellular cohorts and provide the directional cue to the followers [18,21–23,25]. Leader cell formation therefore has critical influences on morphogenesis and wound healing and has been studied both *in vivo* [26,27] and *in vitro* [18,22–24,28,29]. While interfacial geometry plays an important role in regulating leader cell-mediated migration [28,30,31], our recent work has demonstrated the importance of bulk mechanical activity in the emergence of leader cells [23]. Such mechanical activity is associated with a heterogeneous and dynamic increase in the local tension field among follower cells, which further aid the polarization of future leaders. Remarkably, the length scale of leader cell formation—specifically, the separation between two neighbouring leaders—follows the length scale of undulations within the heterogeneous stress field in both normal and chemically perturbed monolayers [23]. While explicit mechanistic relationships between the dynamic heterogeneity in stress field and wound healing remain elusive, this work indicates a connection between them. In addition, another study has previously demonstrated the density dependence of dynamic heterogeneity in form of an increase in jamming and movement correlation upon increasing cell density [13]. Together, these studies suggest that density regulation and dynamic heterogeneity are possibly linked to each other, and that they may have connected implications in cell migration during wound healing. However, while previous reports, including ours, have separately correlated either cell density or dynamic heterogeneity with long-ranged coordination of force and velocity, to the best of our knowledge, no study has yet attempted to unify the effect of these two parameters under a single framework.

In this work, we attempt to examine the quantitative connection between cell density and dynamic heterogeneity and, importantly, the impact of both on collective cell migration during epithelial wound closure. One problem, however, is that neither working cell density nor dynamic heterogeneity is an exact controllable parameter, even if one is able to maintain a precise seeding density to begin with. Therefore, it would be immensely beneficial if a quantity associated with dynamic heterogeneity shows a regular—preferably linear—relationship with cell density, as in that case, for any experimentally obtained value of cell density, the strength of dynamic heterogeneity can be conveniently inferred. In this work, we indeed found one such quantity—the peak height of four-point susceptibility—that shows remarkable linearity across a density range, over many experimental samples, and we call this parameter '*the strength of dynamic heterogeneity*' (SDH). We observed that at low density, when the strength of dynamic heterogeneity is low, cells are not able to coordinate movement and forces with their neighbours. This lack of coordination is clearly reflected in hampered leader–follower behaviour and hence a decreased efficiency of wound healing.

2. Results

(a) Dynamic heterogeneity in the bulk and cell density

We first set out to visualize the dynamics of monolayer heterogeneity with respect to cell density, by measuring the velocities with particle image velocimetry (PIV) and tracing out the cell shapes. To this end, we imaged a Madin–Darby canine kidney (MDCK) epithelial monolayer over several hours in confluent conditions starting from a low-density culture until the cells started dying due to senescence (electronic supplementary material, movie S1) and looked at the morphological and biophysical characteristics. Similar to previous reports [13], the velocity profile of the monolayer showed an enhanced correlated movement as the cell density increased (figure 1*a*(ii)). For morphological analysis, we characterized the cells in distinct structural states: jammed (solid like) and unjammed (fluid like) on the basis of a non-dimensional shape index (q), calculated as the ratio between perimeter and projected cross-sectional area of individual cells, from the captured brightfield images. We additionally compared the brightfield-based segmentation with another segmentation based on the ZO-1 staining of the monolayer and found them to be yielding an almost identical distribution of shape index (electronic supplementary material, figure S1). As explained in the previous works [9,32], jammed cells are characterized by $q < 3.81$ and unjammed cells by $q > 3.81$. Intuitively, at low density, cells displayed very dynamic and unjammed behaviour as depicted by their increased shape indices (figure 1*a*(i), *b*), and the average shape index drops significantly as the cell density increases (figure 1*a*(i),*b*). However, the monolayer maintained both kinetically arrested or jammed and dynamic unjammed populations even when the density increased to a plateau at homeostasis, as observed by the distribution of cellular shape indices and of velocity (figure 1*b*,*c*). Both shape index and velocity data showed considerable variation around the mean value at all densities, as depicted by their coefficients of variation and frequency distribution (figure 1*b*, *c*, insets). Together, these results demonstrated that even at the highest density, the epithelial monolayer maintained a rather heterogeneous population consisting both of kinetically arrested jammed and dynamic unjammed cells.

(b) Finding a quantity linking cell density and dynamic heterogeneity

While the shape and velocity heterogeneity persisted at all densities, we next asked whether the degree of heterogeneity changed as a function of cell density. To this end, we sought analogy of the cellular system with the dense granular matter and applied some of the methods that had been developed to characterize the latter. In granular matter or colloidal suspensions, a very robust method of characterizing spatially heterogeneous dynamics is to find out the trajectory of individual elements and compute the mean square displacement (MSD, Δx^2) and four-point susceptibility (χ_4) [9,33]. While the former represents the degree of caging and active movements, the latter provides a quantitative estimation of the extent to which the dynamics of any two cells are correlated, within a time interval. Thus, while mean square displacement is a reliable metric for cellular movement, four-point susceptibility is more appropriate than MSD for distinguishing

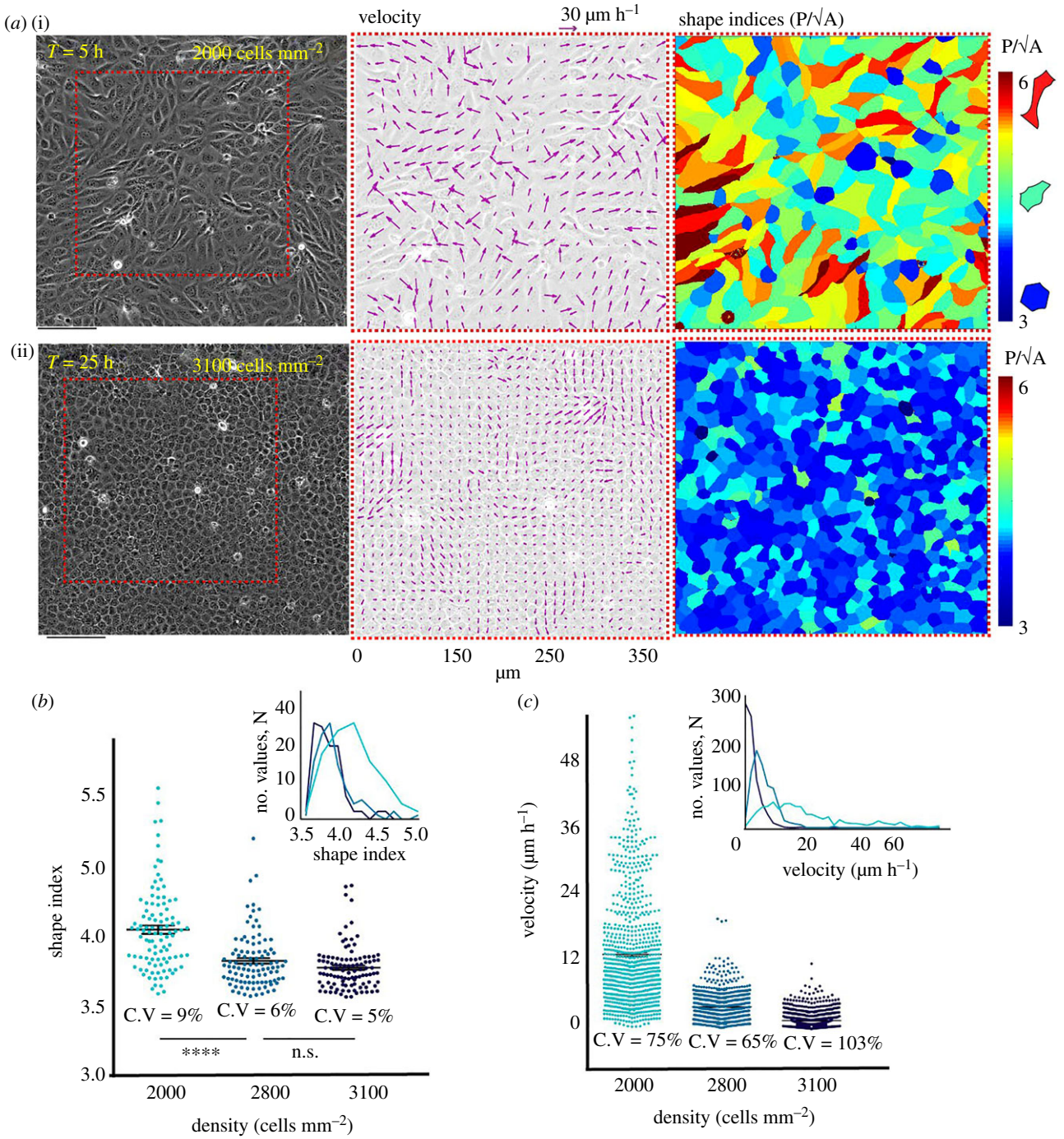

Figure 1. Dynamic heterogeneity at all cell densities. (*a*) Representative phase contrast images (*left panel*), corresponding velocity vectors (*middle panel*) and shape index profiles (*right panel*) at low and high densities showing decrease in overall movement and shape indices as cells become more closely packed. (*b*) Scatter dot plots of cellular shape with increasing densities showing the monolayer maintaining the variability in shape indices even at higher densities. (*c*) Scatter dot plot of velocity with increasing densities showing monolayer maintaining the variability in velocity even at higher densities. Insets of (*b*) and (*c*) show frequency distribution, similar to a Gaussian curve at high density.

correlated motions from the uncorrelated ones. As the cell density increases, and the monolayer approaches the jammed state, the correlation of cellular motions as well as their length and time-scale significantly increase [13]. In such collective context, χ_4 exhibits a peak, whose position approximately represents the average lifetime of the collectively migrating packs, while the height of the peak corresponds roughly to their mean size. Next, to obtain these quantities, we segmented the bright-field images to locate the centroid of each cell (figure 2*a*) and interpolated the values of velocity components, acquired from PIV analysis, to this point and computed the cellular trajectories by integrating the instantaneous velocity field [9] (figure 2*b*). We then computed several related parameters, including effective diffusion coefficient (D_s), from the MSD (figure 2*c*) and position of peak of χ_4 in time as well as its height (figure 2*d*). Among these quantities, the peak height of χ_4 showed an excellent linear relationship with cell density (figure 2*d*(ii)) over several samples. Interestingly, this quantity, by its definition and formulation, represented the strength of both collectivity and dynamic heterogeneity [33] and provided a unique means of connecting dynamic heterogeneity to cell density, in a linear manner. Further, given the robust linear relationship between cell density and peak height of χ_4, which may be called *the strength of dynamic heterogeneity (SDH)*, we mapped a SDH value from the cell density for all our future experiments. In fact, this linear relationship enabled

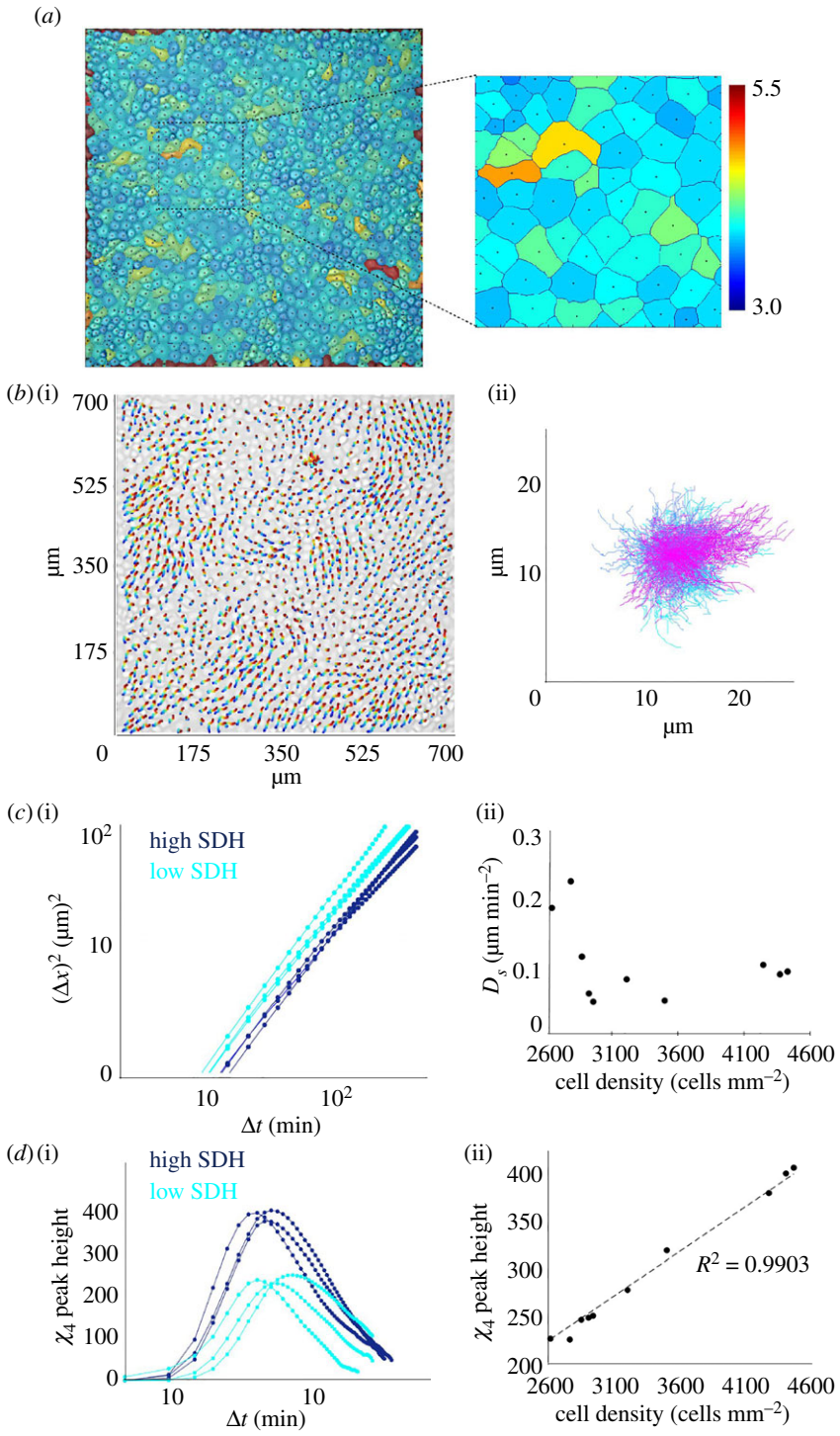

Figure 2. Linking cell density and dynamic heterogeneity. (*a*) Overlapped brightfield and segmented cell boundaries, showing the centroid of each cell. Colours were assigned according to the shape index. (*b*) (i) PIV-derived cellular trajectories, mapped onto the initial brightfield image. (ii) Compilation of all cell trajectories with starting position of every cell set to zero. (*c*) (i) Evolution of mean square displacement (MSD) with time at different cell densities. (ii) Variation of effect diffusion coefficient, as calculated from the graph in (i), with increasing cell density. (*d*) (i) The shape of four-point susceptibility function with respect to time at different cellular densities. (ii) Variation of the peak height of four-point susceptibility function, as calculated from the graph in (i), with increasing cell density. For the linear fit, $R^2 = 0.9903$, implying a high linearity.

us to perceive the dynamics of collective migration in terms of cell density and dynamic heterogeneity, at the same time, interchangeably in a unified framework.

(c) The strength of dynamic heterogeneity and force correlation

Stress profiles of an epithelial sheet display a rugged landscape with peaks and basins defining tensile and compressive stress elements [10], and as we found earlier [23], the distance between neighbouring peaks in the bulk stress landscape, which corresponds to the length scale of long-range force correlation in the epithelial monolayer, correlates with distance between two neighbouring leader cells at the wound margin, in both normal and chemically perturbed monolayers. Given this importance of the stress landscape and force correlation in collective migration, we next examined how the strength of dynamic heterogeneity influenced the force correlation length in epithelia. To this end, we performed traction force microscopy on low- and high-density monolayers to elucidate the

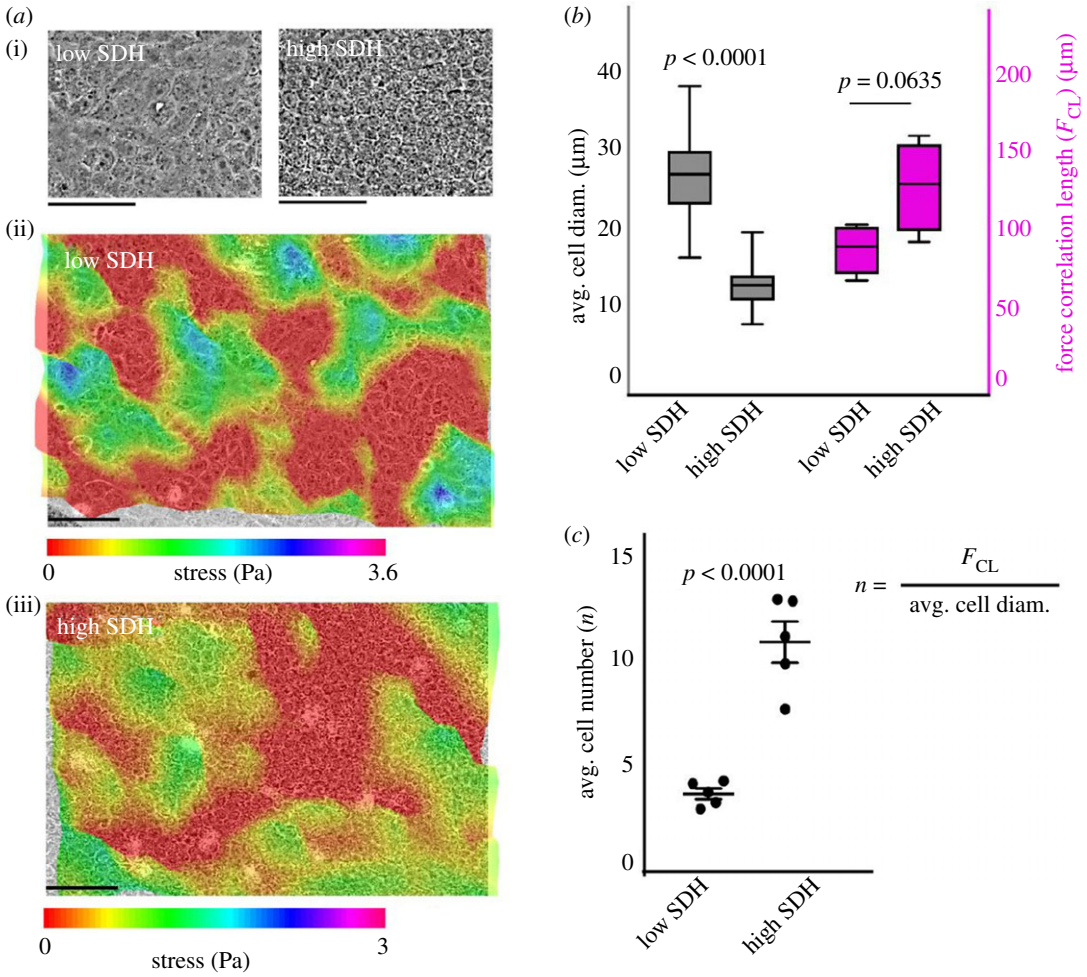

Figure 3. The strength of dynamic heterogeneity influences the force correlation at the multicellular level. (*a*) Representative phase contrast images and stress profile of the monolayers at a representative low and high SDH value. (*b*) Box plots showing average cell diameter (plotted on left *y* axis) and force correlation lengths (plotted on right *y* axis) for low and high SDH, showing no significant difference in correlation lengths. (*c*) Average number of cells correlating force normalized with cell diameter at low and high density showing that cells coordinate much more at higher SDH.

cell–substrate force and to generate the corresponding monolayer stress profile. We grew monolayers of MDCK cells at different densities, and therefore at different SDH values, over a soft polyacrylamide substrate containing fluorescent beads, and computed cellular stresses from the displacement of the beads as described previously. Visually, a densely packed monolayer contained a greater number of cells underneath a stress peak compared to a monolayer with low SDH, indicating higher coordination at high SDH (figure 3*a*(ii,iii)). To quantify the number of cells that were able to integrate their forces with their neighbours, we computed a stress correlation length as described previously [10,21] and divided correlation length by the average cell diameter at low and high SDH, respectively (figure 3*c*). We subsequently found that even though stress correlation lengths showed only slight differences—statistically insignificant—between low and high SDH (figure 3*b*, right *y* axis), the number of cells that were found to coordinate forces was significantly low at lower SDH as compared to a dense monolayer (figure 3*c*). These results are in consensus with the previously reported study showing an increase in the spatial extent of dynamic heterogeneity when the cells pack together [13].

(d) Dynamic heterogeneity and efficiency of wound closure

Next, to understand the possible implications of different magnitudes of dynamic heterogeneity with respect to the efficiency of epithelial wound healing, we performed a confinement-release wound healing experiment at low and high SDH. To this end, we grew monolayers of MDCK cells within confined areas and then lifted off the confinement to prompt two-dimensional sheet-like migration as described previously [18,23,24]. We then followed the temporal evolution of the wound margin and acquired diverse kinematic information associated with the marginal cells. To this end, we individually marked the cells at the wound margin, both leader and non-leader cells, and followed their movements over time (figure 4*a*,*b*). Interestingly, the results revealed that in monolayer at low SDH, even though most of the cells are highly dynamic within the bulk (figure 1*a*), wound healing is much slower than in the monolayer at high SDH (figure 4*a*, electronic supplementary material, movie S2). Upon plotting the coordinates of individual cell tracks on an *x*,*y* plane over 6 h, we observed sharp differences between cells at low and high SDH. At high SDH, cells migrated towards the wound much more efficiently, with seldom changes in direction, with leader cells oving consistently towards the direction of migration indicating their role in guiding the followers. However, at low SDH, both leader and follower cells frequently change direction and the migration seems less efficient (figure 4*b*, electronic supplementary material, movie S2). In order to quantify these differences, we computed average persistence and average velocity of migration. For a given cell track, at a given instant of time, directional persistence is

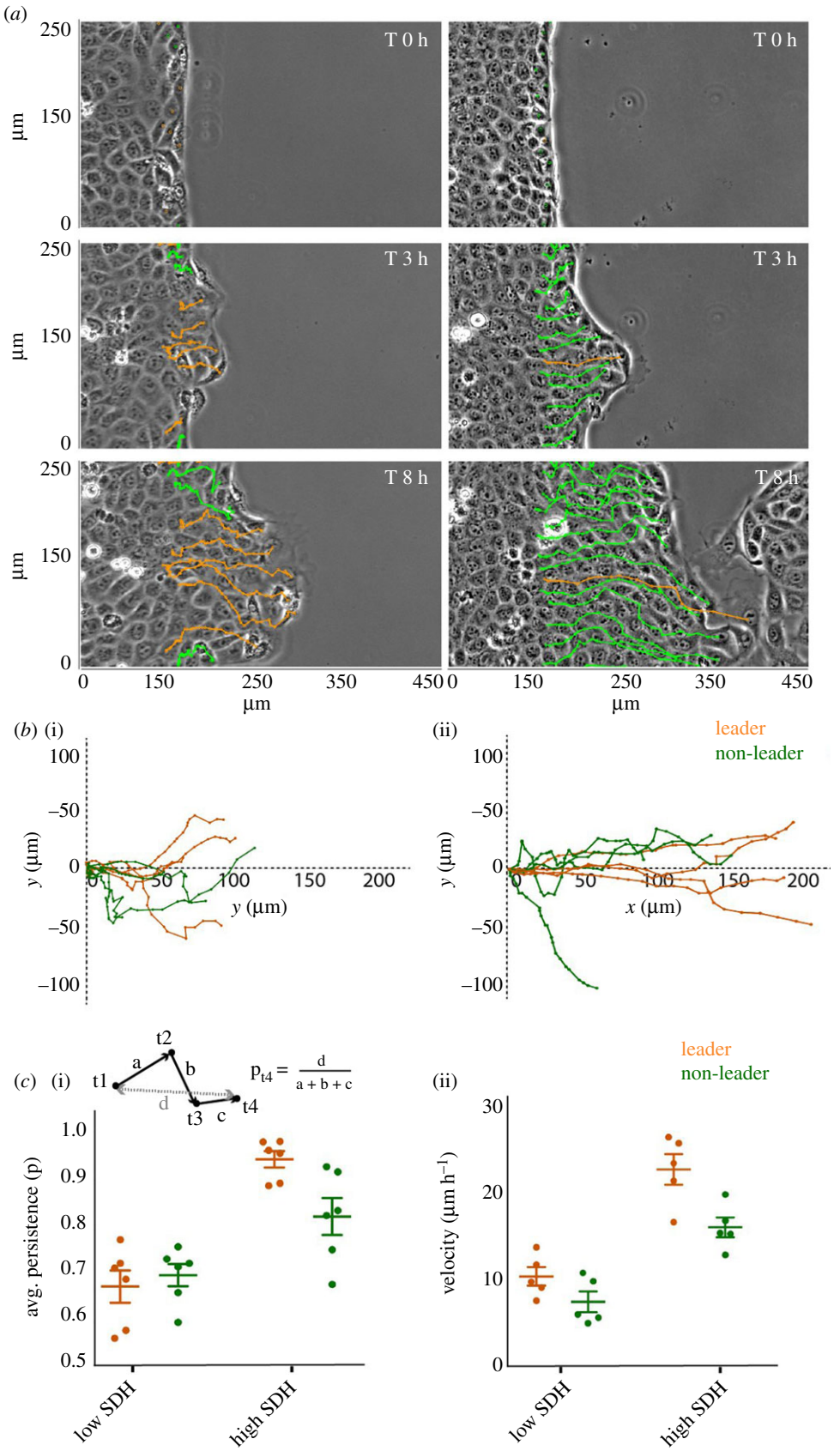

Figure 4. Efficient wound closure and dynamic heterogeneity. (*a*) Representative phase contrast images and corresponding leader and non-leader cell tracks in monolayers at low and high SDH scenarios, showing wound closure is much slower at lower SDH. (*b*) Representative individual cell tracks of leader and non-leader cells at low (i) and high (ii) SDH, showing cells migrating much further at higher SDH. (*c*) Average cellular persistence (i) and average velocity (ii) at low and high density showing both leaders and non-leader cells are more persistent and migrate faster at high SDH. Further, leader cells showed significantly higher persistence and higher velocity than non-leaders at high SDH, while at low SDH, difference between leaders and non-leaders was found to be insignificant.

defined as the ratio of end-to-end distance and total accumulated distance of the track (figure 4*c*(i), inset). Remarkably, we found out that at low SDH, both leader and follower cells are less persistent and migrate much slower as compared to cells at high SDH (figure 4*c*). Interestingly, while at low SDH, there is no significant difference between kinematics of leader and

follower cells, at high SDH, leaders show a higher persistence and higher velocity as compared to the non-leaders, indicating the ability of leader cells to guide the migration (figure 4*c*). Taken together, these results demonstrated the importance of high dynamic heterogeneity in the bulk monolayer for efficient wound closure and for its related dynamics at the wound interface. They also showed that migration became persistent and faster when cells were packed at high density, and therefore, possessed high dynamic heterogeneity. Furthermore, persistent migration of leader cells at higher heterogeneity indicated efficient leader–follower-mediated collective migration, which seemed to be lost at low heterogeneity.

(e) Dynamics of cellular adhesions show impaired leader–follower behaviour at low heterogeneity

We then asked why the wound closure might be slower and less persistent at low SDH. Collective migration crucially depends on cellular ability to exert traction forces onto the underlying substrate or to the extracellular matrix through focal adhesion points. Dynamic regulation of the size, shape and orientation of the cell-matrix adhesion is often a prerequisite for effective migration. Intriguingly, we know very little about how the individual focal adhesions are redistributed and reoriented during collective cell migration. By conventional means, examining the focal adhesions in real time would require stable expression of a fluorescent protein-tagged focal adhesion protein in all cells. However, this manipulation would perturb the collective system, and the inherent genetic noise would cause local variability in the expression level, further distorting the traction field. To circumvent these problems, here we used a non-invasive optical technique called reflection interference contrast microscopy (RICM) [34], which delineated cell–substrate adhesion points as dark spots (figure 5*a*). RICM did not require any genetic manipulation and, hence, eliminated any active interference with the system. To this end, we first validated the fidelity of the RICM-based detection of focal adhesion points by an overlapping analysis of the dark spots from RICM and immunostaining of paxillin molecules (figure 5*b*), which showed excellent correspondence as confirmed by the high correlation coefficient (figure 5*c*). Next, upon analysing the relative orientation of focal adhesions with respect to the average direction of the collective migration at any point of time at low and high SDH (figure 5*d*,*e*), we observed a few important trends. At high SDH, when the wound healing was efficient, the focal adhesions of the leader cells displayed high orientation bias towards the average direction of migration while the remaining non-leader cells had their focal adhesions inclined towards the nearest leader (figure 5*d*(iv-vi),*e*(ii)). On the other hand, at lower density, when the wound healing efficiency appeared reduced, the orientation bias of leader cells seemed to be missing and there was no significant difference between focal adhesion orientation in leader and non-leader cells (figure 5*d*(i-iii),*e*(ii)), indicating the leader cells lost the sense of direction when the dynamic heterogeneity was low. Together, these results demonstrated how the strength of dynamic heterogeneity correlated with the ability of cells to align and migrate in the right direction and highlighted the impaired sense of orientation and loss of leader–follower behaviour at low dynamic heterogeneity value.

3. Discussion

To summarize, in a background where previous reports had approached the problem of large-range correlation in motion and force among epithelial cells from the point of view of either dynamic heterogeneity or cell density, we provided a unified view. We showed that the cell density and a representative quantity of dynamic heterogeneity—SDH—were linearly related to each other and that the strength of heterogeneity determined the efficiency of collective migration of cells. Specifically, at higher SDH, cells were able to coordinate their movement as well as their forces much more when compared to the cells at lower SDH. Subsequently, a monolayer at high SDH was able to heal a wound much faster in comparison to those at lower heterogeneity or density. Further, our RICM-based tracking of cell–substrate adhesions in live cells showed that the collective migration involving leader–follower behaviour was much more prominent at higher SDH values. This observation implied that while leader cells oriented their focal adhesions towards the wound at all SDH, at high SDH, followers were more likely to orient their focal adhesions towards the leaders, thereby allowing them to follow the latter, than at low SDH. Such leader–follower behaviour had previously been shown to increase the efficiency of collective migration [18,21,22] and was found critical in healing larger wounds where cells are supposed to cover long distances via migration [29,31]. In this respect, given that cell–cell junctions mature and stabilize with the increasing cell density, it becomes tempting to speculate whether the spontaneous dynamic heterogeneity in motion and force, the strength of which amplifies with increasing density, actually helps in maintaining a balanced state of motility and cohesion, to maximize the efficiency of collective migration and wound closure. In the past, many studies had described density regulation at epithelial homeostasis and several molecular pathways through which this regulation could be achieved [5,35–39]. However, the implications of cell density in the context of dynamic heterogeneity and its impact on wound healing remained elusive. At this point, having established the required implication, we may wonder whether all or any of those pathways may provide the molecular mechanism explaining the linear-linkage between cell density and dynamic heterogeneity and how they affect the process of collective migration. We hope that these speculations will lead to several important biological or molecular investigations in the future. Nevertheless, there are certain *in vivo* implications of our study that cannot be overlooked. There are many ways wound healing and unjamming may take place at different densities *in vivo*. For example, cell density of lens epithelium [40] and corneal endothelium [41] decreases significantly with age. Also, epithelium persistently exposed to drugs and infection shows a lower cell density than healthy epithelium [42]. In asthma, bronchoconstriction and ensuing hyper-contraction of the bronchial epithelium result in the loss of cells, known as epithelial denuding [43]. In all of these cases, as implied by our study, an aged or affected individual should show predictively lower efficiency of wound healing than a healthy individual. Lastly, a previous study on the unjamming in bronchial epithelium [9] found homeostatic cell densities varying by as much as 12% from donor to donor. How that kind of population level heterogeneity eventually influences the health of an individual remains to be answered.

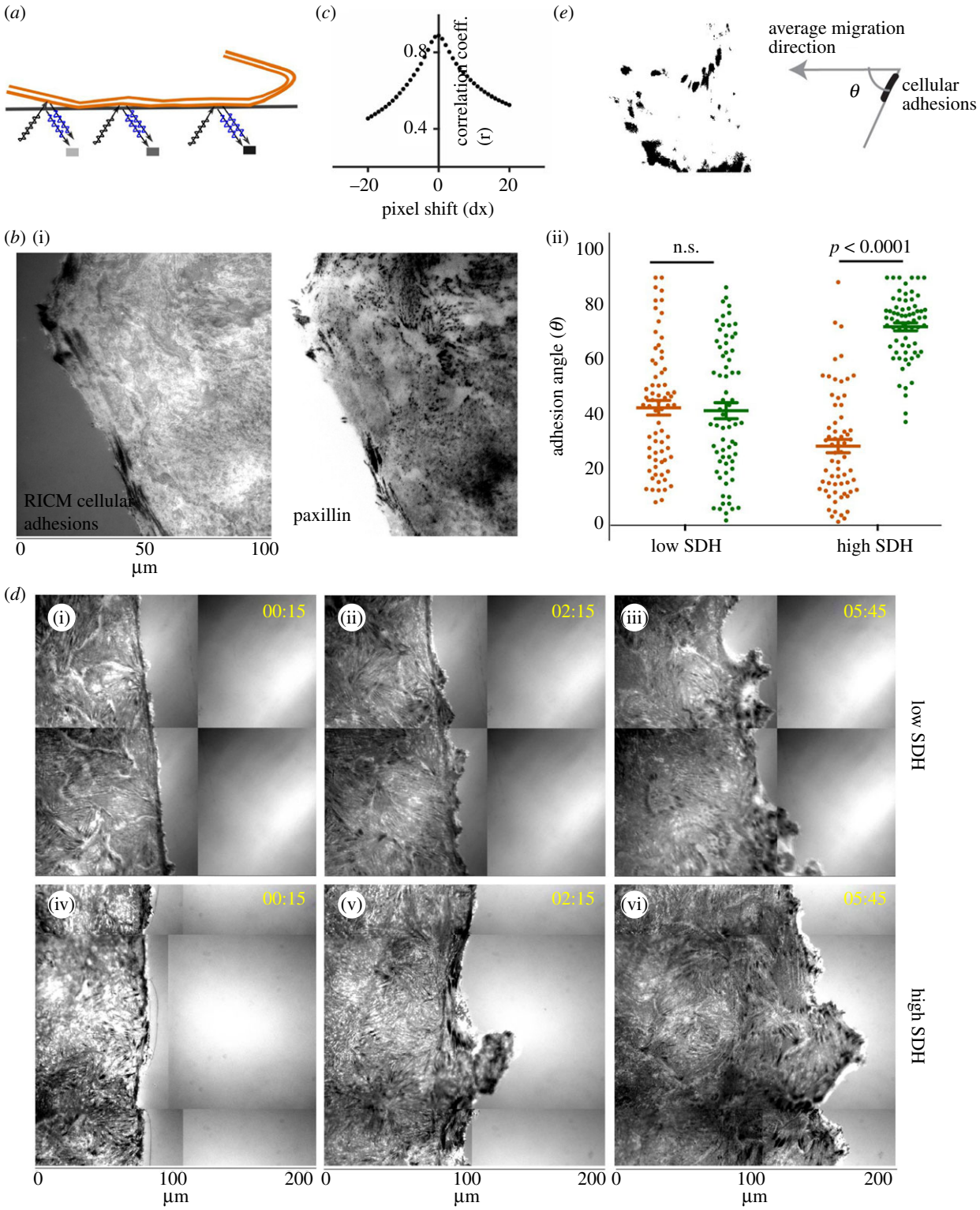

Figure 5. Cellular adhesion patterns at low and high dynamic heterogeneity. (*a*) Schematic representation of Reflection Interference Contrast Microscopy (RICM) for measuring dynamic cellular adhesions. (*b*) Cellular adhesions as measured by RICM (i) and focal adhesions from paxillin staining (ii). (*c*) Colocalization analysis using the Pearson correlation coefficient showing RICM adhesions colocalized with focal adhesions, as stained with an antibody against paxillin. (*d*) Representative time lapse images of cellular adhesions at low and high SDH showing leaders orient towards the direction of migration and non-leaders towards the leader cell at SDH. (*e*) Scatter dot plot of focal adhesion orientation angles in leader and non-leader cells with respect to the direction of migration.

Finally, from a physical perspective, recent technical and computational advances have allowed biophysicists to describe physical behaviour of epithelia using mesoscale principles [44]. The mesoscale approach, which is ideally not concerned with microscopic details such as structural and molecular changes within single cells, provides an analogy to a glassy solid or dense particulate matter and aspires to equate the observed dynamic heterogeneity in epithelial monolayers with that in dense colloidal particles. Extrapolating that analogy, we may wonder here whether a similar linear relationship between particle density and SDH also exists in colloidal systems. However, before such extrapolation, we must consider that there is a crucial difference between these two scenarios. While in the colloidal system, we may expect dynamic heterogeneity to grow with an increasing packing fraction of particles, in the confluent space-filling epithelial

monolayer, the packing fraction is always one, and cell density increases due to cell division. While physical studies in future will have to take this crucial difference due to cell division into account, we presume that the present work opens up new research possibilities encompassing both biochemistry and biophysics of wound healing in the epithelial tissue.

4. Methods

Please see the detailed materials and methods in the electronic supplementary material document.

Data accessibility. This article has no additional data.

Authors' contributions. M.V., J.P.S. and T.D. conceived the project. M.V. and B.T. performed experiments. M.V., B.T. and T.D. analysed the results. M.V. and T.D. wrote the manuscript. All authors agreed on the manuscript as in the submitted version.

Competing interest. The authors declare no competing financial interest.

Funding. T.D. and B.T. sincerely acknowledge funding from the Max Planck Society as well as Department of Atomic Energy (DAE), Government of India towards supporting this project. M.V. acknowledges funding support from Win-Kolleg, Heidelberg Academy of Sciences. This study was in part supported by the intramural funds of Tata Institute of Fundamental Research Hyderabad.

Acknowledgement. We would like to thank I-Hsuan Wang and Aravind H for their useful contributions. T.D. is a partner group leader of the Max Planck Society (MPG), Germany. M.V. is a guest scientist at Max Planck Institute for Medical Research, Heidelberg and acknowledges support from School of Cellular and Molecular Medicine, University of Bristol. J.P.S. is the Weston Visiting Professor at the Weizmann Institute of Science and a member of the cluster of excellence CellNetworks at Heidelberg University.

References

1. Marchiando AM, Graham WV, Turner JR. 2010 Epithelial barriers in homeostasis and disease. *Annu. Rev. Pathol.* **5**, 119–144. (doi:10.1146/annurev.pathol.4.110807.092135)
2. Shashikanth N, Yeruva S, Ong MLDM, Odenwald MA, Pavlyuk R, Turner JR. 2017 Epithelial organization: the gut and beyond. *Compr. Physiol.* **7**, 1497–1518. (doi:10.1002/cphy.c170003)
3. Haeger A, Wolf K, Zegers MM, Friedl P. 2015 Collective cell migration: guidance principles and hierarchies. *Trends Cell Biol.* **25**, 556–566. (doi:10.1016/j.tcb.2015.06.003)
4. Friedl P, Gilmour D. 2009 Collective cell migration in morphogenesis, regeneration and cancer. *Nat. Rev. Mol. Cell Biol.* **10**, 445–457. (doi:10.1038/nrm2720)
5. Macara IG, Guyer R, Richardson G, Huo Y, Ahmed SM. 2014 Epithelial homeostasis. *Curr. Biol.* **24**, R815–R825. (doi:10.1016/j.cub.2014.06.068)
6. Park JA, Atia L, Mitchel JA, Fredberg JJ, Butler JP. 2016 Collective migration and cell jamming in asthma, cancer and development. *J. Cell Sci.* **129**, 3375–3383. (doi:10.1242/jcs.187922)
7. Sadati M, Taheri Qazvini N, Krishnan R, Park CY, Fredberg JJ. 2013 Collective migration and cell jamming. *Differentiation* **86**, 121–125. (doi:10.1016/j.diff.2013.02.005)
8. Haeger A, Krause M, Wolf K, Friedl P. 2014 Cell jamming: collective invasion of mesenchymal tumor cells imposed by tissue confinement. *Biochim. Biophys. Acta* **1840**, 2386–2395. (doi:10.1016/j.bbagen.2014.03.020)
9. Park JA *et al.* 2015 Unjamming and cell shape in the asthmatic airway epithelium. *Nat. Mater.* **14**, 1040. (doi:10.1038/NMAT4357)
10. Tambe DT *et al.* 2011 Collective cell guidance by cooperative intercellular forces. *Nat. Mater.* **10**, 469–475. (doi:10.1038/NMAT3025)
11. Hardin C *et al.* 2013 Glassy dynamics, cell mechanics, and endothelial permeability. *J. Phys. Chem. B* **117**, 12 850–12 856. (doi:10.1021/jp4020965)
12. Angelini TE, Hannezo E, Trepat X, Fredberg JJ, Weitz DA. 2010 Cell migration driven by cooperative substrate deformation patterns. *Phys. Rev. Lett.* **104**, 168104. (doi:10.1103/PhysRevLett.104.168104)
13. Angelini TE, Hannezo E, Trepat X, Marquez M, Fredberg JJ, Weitz DA. 2011 Glass-like dynamics of collective cell migration. *Proc. Natl Acad. Sci. USA* **108**, 4714–4719. (doi:10.1073/pnas.1010059108)
14. Trepat X, Wasserman MR, Angelini TE, Millet E, Weitz DA, Butler JP, Fredberg JJ. 2009 Physical forces during collective cell migration. *Nat. Phys.* **5**, 426–430. (doi:10.1038/nphys1269)
15. Saw TB *et al.* 2017 Topological defects in epithelia govern cell death and extrusion. *Nature* **544**, 212–216. (doi:10.1038/nature21718)
16. Mongera A *et al.* 2018 A fluid-to-solid jamming transition underlies vertebrate body axis elongation. *Nature* **561**, 401–405. (doi:10.1038/s41586-018-0479-2)
17. Malinverno C *et al.* 2017 Endocytic reawakening of motility in jammed epithelia. *Nat. Mater.* **16**, 587–596. (doi:10.1038/nmat4848)
18. Poujade M, Grasland-Mongrain E, Hertzog A, Jouanneau J, Chavrier P, Ladoux B, Buguin A, Silberzan P. 2007 Collective migration of an epithelial monolayer in response to a model wound. *Proc. Natl Acad. Sci. USA* **104**, 15 988–15 993. (doi:10.1073/pnas.0705062104)
19. Tarle V, Ravasio A, Hakim V, Gov NS. 2015 Modeling the finger instability in an expanding cell monolayer. *Integr. Biol.* **7**, 1218–1227. (doi:10.1039/c5ib00092k)
20. Hakim V, Silberzan P. 2017 Collective cell migration: a physics perspective. *Rep. Prog. Phys.* **80**, 076601. (doi:10.1088/1361-6633/aa65ef)
21. Petitjean L, Reffay M, Grasland-Mongrain E, Poujade M, Ladoux B, Buguin A, Silberzan P. 2010 Velocity fields in a collectively migrating epithelium. *Biophys. J.* **98**, 1790–1800. (doi:10.1016/j.bpj.2010.01.030)
22. Reffay M, Parrini MC, Cochet-Escartin O, Ladoux B, Buguin A, Coscoy S, Amblard F, Camonis J, Silberzan P. 2014 Interplay of RhoA and mechanical forces in collective cell migration driven by leader cells. *Nat. Cell Biol.* **16**, 217–223. (doi:10.1038/ncb2917)
23. Vishwakarma M, Di Russo J, Probst D, Schwarz US, Das T, Spatz JP. 2018 Mechanical interactions among followers determine the emergence of leaders in migrating epithelial cell collectives. *Nat. Commun.* **9**, 3469. (doi:10.1038/s41467-018-05927-6)
24. Das T, Safferling K, Rausch S, Grabe N, Boehm H, Spatz JP. 2015 A molecular mechanotransduction pathway regulates collective migration of epithelial cells. *Nat. Cell Biol.* **17**, 276–287. (doi:10.1038/ncb3115)
25. Rorth P. 2012 Fellow travellers: emergent properties of collective cell migration. *EMBO Rep.* **13**, 984–991. (doi:10.1038/Embor.2012.149)
26. Bianco A *et al.* 2007 Two distinct modes of guidance signalling during collective migration of border cells. *Nature* **448**, 362–365. (doi:10.1038/nature05965)
27. Montell DJ, Yoon WH, Starz-Gaiano M. 2012 Group choreography: mechanisms orchestrating the collective movement of border cells. *Nat. Rev. Mol. Cell Biol.* **13**, 631–645. (doi:10.1038/nrm3433)
28. Rausch S, Das T, Soiné JRD, Hofmann TW, Boehm CHJ, Schwarz US, Boehm H, Spatz JP. 2013 Polarizing cytoskeletal tension to induce leader cell formation during collective cell migration. *Biointerphases* **8**, 32. (doi:10.1186/1559-4106-8-32)
29. Anon E, Serra-Picamal X, Hersen P, Gauthier NC, Sheetz MP, Trepat X, Ladoux B. 2012 Cell crawling mediates collective cell migration to close undamaged epithelial gaps. *Proc. Natl Acad. Sci. USA* **109**, 10 891–10 896. (doi:10.1073/pnas.1117814109)
30. Vedula SR, Leong MC, Lai TL, Hersen P, Kabla AJ, Lim CT, Ladoux B. 2012 Emerging modes of collective cell migration induced by geometrical constraints. *Proc. Natl Acad. Sci. USA* **109**, 12 974–12 979. (doi:10.1073/pnas.1119313109)
31. Ravasio A *et al.* 2015 Gap geometry dictates epithelial closure efficiency. *Nat. Commun.* **6**, 7683. (doi:10.1038/ncomms8683)

32. Bi DP, Lopez JH, Schwarz JM, Manning ML. 2015 A density-independent rigidity transition in biological tissues. *Nat. Phys.* **11**, 1074. (doi:10.1038/NPHYS3471)
33. Keys AS, Abate AR, Glotzer SC, Durian DJ. 2007 Measurement of growing dynamical length scales and prediction of the jamming transition in a granular material. *Nat. Phys.* **3**, 260–264. (doi:10.1038/nphys572)
34. Limozin L, Sengupta K. 2009 Quantitative reflection interference contrast microscopy (RICM) in soft matter and cell adhesion. *ChemPhysChem* **10**, 2752–2768. (doi:10.1002/cphc.200900601)
35. Lu L *et al.* 2013 LRIG1 regulates cadherin-dependent contact inhibition directing epithelial homeostasis and pre-invasive squamous cell carcinoma development. *J. Pathol.* **229**, 608–620. (doi:10.1002/path.4148)
36. Katoh H, Fujita Y. 2012 Epithelial homeostasis: elimination by live cell extrusion. *Curr. Biol.* **22**, R453–R455. (doi:10.1016/j.cub.2012.04.036)
37. Eisenhoffer GT, Loftus PD, Yoshigi M, Otsuna H, Chien C-B, Morcos PA, Rosenblatt J. 2012 Crowding induces live cell extrusion to maintain homeostatic cell numbers in epithelia. *Nature* **484**, 546–549. (doi:10.1038/nature10999)
38. Gudipaty SA, Lindblom J, Loftus PD, Redd MJ, Edes K, Davey CF, Krishnegowda V, Rosenblatt J. 2017 Mechanical stretch triggers rapid epithelial cell division through Piezo1. *Nature* **543**, 118–121. (doi:10.1038/nature21407)
39. Liu Y, Xu G-K, Zhang L-Y, Gao H. 2019 Stress-driven cell extrusion can maintain homeostatic cell density in response to overcrowding. *Soft Matter* **15**, 8441–8449. (doi:10.1039/c9sm01219b)
40. Oharazawa H, Ibaraki N, Matsui H, Ohara K. 2001 Age-related changes of human lens epithelial cells in vivo. *Ophthalmic Res.* **33**, 363–366. (doi:10.1159/000055694)
41. Joyce NC. 2003 Proliferative capacity of the corneal endothelium. *Prog. Retin. Eye Res.* **22**, 359–389. (doi:10.1016/S1350-9462(02)00065-4)
42. Puliafito A, Primo L, Celani A. 2017 Cell-size distribution in epithelial tissue formation and homeostasis. *J. R. Soc. Interface* **14**, 20170032. (doi:10.1098/rsif.2017.0032)
43. Knight DA, Holgate ST. 2003 The airway epithelium: structural and functional properties in health and disease. *Respirology* **8**, 432–446. (doi:10.1046/j.1440-1843.2003.00493.x)
44. Trepat X, Sahai E. 2018 Mesoscale physical principles of collective cell organization. *Nat. Phys.* **14**, 671–682. (doi:10.1038/s41567-018-0194-9)